Journal of Engineering and Sustainable Development
Vol. 30, No. 02, March 2026
https://jeasd.uomustansiriyah.edu.iq/index.php/jeasd
ISSN 2520-0917
Research Article
https://doi.org/10.31272/jeasd.2133

Partial Replacement of Cement with Agricultural Waste (Palm Ash) to Improve the Concrete Properties

Safa Alqeisi*, Ali H. Nahhab

Department of Civil Engineering, Babylon University, Babylon, Iraq

*Email: eng980.safa.ali@student.uobabylon.edu.iq

Article Info

Received	**08/08/2024**
Revised	**15/01/2026**
Accepted	**16/01/2026**

Abstract

Recently, many pozzolanic materials resulting from industrial and agricultural wastes, such as palm ash, have been used to improve the properties of concrete and reduce cement use. This research investigated the preparation and replacement of palm ash by the weight of cement and its impact on the properties of fresh and hardened concrete. Two types of palm ash, namely palm frond ash (PFA) and palm frond base ash (PFBA), were prepared using fronds and frond bases. The replacement proportions for each type of palm ash were 0%, 5%, 10%, 15%, and 20% by weight of cement. The results indicated that the initial and final setting times increased, and the slump of the concrete decreased as the content of PFA and PFBA increased. The compressive, splitting, tensile strength, and static modulus of elasticity of PFA and PFBA-concrete improved with curing at 7, 28, and 90 days, with the 5% replacement. Higher ash inclusion reduced the mechanical properties at early ages. The development of strength with age was evident in the scanning electron microscope (SEM) images, where the microstructure of PFA20 was denser than that of the control mix. Except for the 5% PFA replacement, all other mixtures exhibited slightly higher water absorption.

Keywords: Compressive strength; Durability; Modulus of elasticity; Palm Frond Ash

1. Introduction

In many developing countries, the disposal of agricultural waste poses a significant challenge as it contributes to environmental degradation and necessitates the allocation of extensive land for landfills. A viable solution to these issues involves recycling this waste through controlled incineration and utilizing the resulting ash for more valuable purposes [1]. Utilizing such waste materials as substitutes for cement in concrete production has the potential to decrease production costs and mitigate the adverse environmental effects associated with waste disposal. It's worth noting that the cement industry is accountable for approximately 5% of global CO_2 emissions and contributes to environmental pollution [2].

To reduce CO_2 emissions, researchers have proposed several solutions, as follows:

- Using Supplementary Cementitious Materials (SCMs) involves partially substituting conventional cement with materials derived from agricultural, industrial, or natural waste sources. SCMs encompass a variety of materials, including metakaolin, natural pozzolan, palm oil fuel, ash, rice husk, fly ash, and steel slag.
- Advancing Geopolymer Concrete: Researchers are exploring the development of geopolymer concrete as a more sustainable alternative.
- Fuel Source Substitution and Clinker Production Modification: Investigating the substitution of fuel sources and making alterations to the clinker production process to minimize carbon emissions [3].

Palm ash (PA) is considered a pozzolanic material with a substantial content of silica and alumina. When exposed to moisture, it undergoes a reaction with ($Ca(OH)_2$) to produce C-S-H, which plays a pivotal role in enhancing the strength of concrete and improving its properties [4]. The following equations show the interactions related to the palm ash [5]:

$$Ca(OH)_2 \rightarrow Ca^{2+} + 2OH^- \quad (1)$$

$$Si - O - Si + 3OH^- \rightarrow [SiO(OH)_3]^- \quad (2)$$

$$Si - O - Al + 7OH^- \rightarrow [SiO(OH)_3]^- + [Al(OH)_4]^- \quad (3)$$

$$[SiO(OH)_3]^- + Ca^{2+} + H_2O + OH^- \rightarrow C - S - H \quad (4)$$

$$2[Al(OH)_4]^- + 4Ca^{2+} + 6H_2O + 6OH^- \rightarrow C_4AH_{13} \quad (5)$$

There are several factors that affect the effectiveness of pozzolanic materials, including the fineness of the pozzolanic material, surface area, chemical composition, burning temperature, carbon and sulfate content, hydrogen ion concentration, and the age of the concrete [5]. The greater the fineness of the pozzolanic material, the greater its effectiveness for interaction, and thus improving the durability, packing density, and strength of concrete [6].

PA has an effect on the properties of concrete when it is partially replaced with cement, including delaying the initial and final setting times. This delay becomes more significant as the percentage of replacement increases. Also, the lower the fineness of the ash, the greater the effect of the ash on delaying the setting time because the large particles of ash enhance the ratio of water/binder in the concrete mixture [7]. Oyejobi et al. [1] studied the workability of concrete using the slump test with (0%, 10%, 20%, and 30%) replacement, and the results showed that the height of the slump decreased as the percentage of PA replacement increased. This is because palm ash absorbs more water, resulting in a paste of standard consistency compared to cement.

For the hardened properties of concrete, Hamada et al. [8] found that incorporating PA into concrete mixes resulted in enhanced compressive strength over time. This improvement was attributed to the robust pozzolanic reaction of palm ash when compared to using only ordinary Portland cement (OPC). The substantial presence of SiO_2 in palm ash played a significant role in amplifying the pozzolanic reaction, consequently enhancing the mechanical properties in concrete mixtures.

From the microstructural analysis, it was found that the reason for the increase in compressive strength was due to the effect of filling voids, as well as the formation of more C-S-H from the interaction of the pozzolanic material with $Ca(OH)_2$ [9]. Chinnu et al. [10] found that the splitting tensile strength was greater than that of the control mix when the replacement rate was low, but it decreased when the replacement rate exceeded 20%. It is well-known that the modulus of elasticity of normal-weight concrete is related to the compressive strength of the concrete. Increasing the hydration rate leads to densification of the concrete's texture, resulting in an increase in concrete stiffness [11].

Thomas et al. [12] indicated that the ash replacement of 20% gave an excellent modulus of elasticity at the age of one year, and this was due to the association resulting from PA that occurs between the paste and the aggregate. Hadi et al.[13] demonstrated that PA25 exhibited lower water absorption and sorptivity than the control mix. This phenomenon is attributed to the filler effect induced by PA particles in the paste, which reduces the number of pores. However, water absorption and sorptivity readings increased with higher PA content beyond 25%. This increase can be attributed to the greater water demand, leading to an increase in pores within the paste. Over time, these readings decreased due to the pozzolanic reaction between PA and cement particles, resulting in a denser and less porous paste.

This research used two types of palm ash made from the waste of the adjacent palm date tree, which is easily accessible, as a partial replacement for cement in concrete. It also monitored the concrete's strength and durability tests to ascertain whether employing palm ash in concrete manufacture is feasible.

2. Experimental Work

2.1. Materials

2.1.1. Cement

In this study, Ordinary Portland cement class CEM I 32.5 R was used, which meets the requirement of IQS No. 5 [14]. Specific gravity of 3.15 g/cm^3 and Blaine fineness of 315 m^2/kg.

2.1.2. aggregate

Local natural sand with a maximum particle size of (4.75) mm, a fine modulus of 2.8, sulfate content of 0.2%, and a specific gravity of 2.6, conforming to the requirements of IQS No. 45 [15], was used as fine aggregate.

The grading of fine aggregate is demonstrated in Fig. 1.

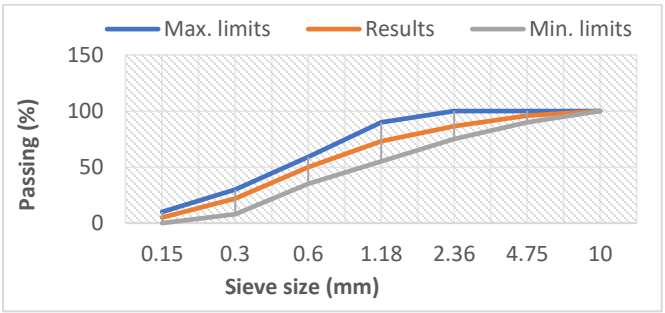

Figure 1. Fine aggregates grading

The coarse aggregate used was crushed gravel with a maximum size of 19 mm, with a sulfate content of 0.03% and a specific gravity of 2.7. It conformed to the requirements of IQS No. 45[15]. The coarse aggregate grading process is demonstrated in Fig. 2.

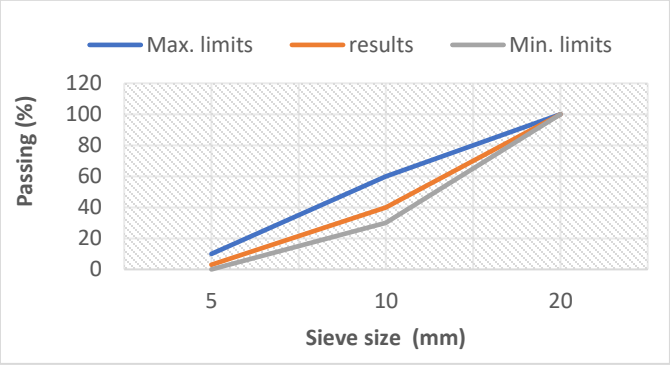

Figure 2. Coarse aggregates grading

2.1.3. Palm Ash

Palm ash, shown in Fig. 3, was prepared by burning dry palm fronds and palm frond base fibres. After the combustion process was completed, the resulting ash was sieved through a No. 30

mesh to remove incompletely burned fibres. Subsequently, it was subjected to further burning in an oven at a temperature of 700 degrees for one hour to eliminate any remaining carbon that didn't burn completely. After cooling, the ash was ground and passed through sieve No. 200 (75µm). Samples were collected from both types of ash, PFA and PFBA, to evaluate their chemical composition using the X-ray fluorescence (EDX) technique.

(a) (b)

Figure 3. (a) Palm frond ash sieved No. 200

(b) Palm frond base ash sieved No. 200

The specific gravity of PFA and PFBA was also determined according to ASTM C188[16] by filling the graduated cylinder to 120 ml with kerosene, then adding 20 g of ash and mixing it well with a glass rod. The mix was left for a while, and then the reading was taken, and then the specific gravity was determined according to the following equation:

$$Specific\ Gravity = \frac{w}{v1-v2} \quad (6)$$

w = weight of ash (Kg)

v1= volume of kerosene (m^3)

v2 = volume of mixing (kerosene + ash) (m^3)

The chemical and physical properties are presented in Table 1.

Table 1. Chemical and Physical properties of palm frond ash PFA and palm frond base ash PFBA

Oxide	PFA (%)	PFBA (%)
SiO_2	35.61	24.32
Al_2O_3	2	1.09
Fe_2O_3	1.22	0.42
CaO	15.28	10.66
MgO	5.85	9.13
SO_3	1.76	2.85
Na_2O	6.2	8.4
K_2O	9.27	10.8
Cl	6	8
P_2O_5	2.2	3.4
CuO	1.9	2.1
Loss of ignition (LOI)	12.68	18.77
specific gravity (Kg/m^2)	2.5	2.85
Blaine's fineness (m^2/ kg)	480	505

2.2 Experimental Procedure

The control mix was designed according to the American code ACI 211.1 [17], with a targeted slump range of (80-100) mm and a water-to-cement (w/c) ratio of 0.45. Cement was substituted with palm frond ash and palm frond base ash at various levels: 5%, 10%, 15%, and 20% by weight relative to the total cement weight. The superplasticizers (SP) dosage was used to achieve the required slump in mixes, in which ash replaced cement. The specific mixture proportions can be found in Table 2.

3. Test Methods

3.1. Setting Time Test

These test methods determine the time of setting hydraulic cement using the Vicat apparatus according to ASTM C 187 [18] and ASTM C191 [19]. Fig. 4 shows the testing procedure of the setting time used in the current study.

Table 2. Mix properties

Mix	Cement (Kg/m^3)	Palm ash (Kg/m^3)	Sand (Kg/m^3)	Gravel (Kg/m^3)	SP (%)	Water (Kg/m^3)
OR	456	-----	730	998	-----	162
PFA5	433	23	726	998	0.1	162
PFA10	410	64	723	998	0.2	162
PFA15	388	69	716	998	0.3	162
PFA20	365	91	709	998	0.5	162
PFBA5	433	23	729	998	0.1	162
PFBA10	410	64	727	998	0.2	162
PFBA15	388	68	725	998	0.3	162
PFBA20	365	91	723	998	0.5	162

*Where:(**OR**): control mix, (**PFA**): palm frond ash concrete, (**PFBA**): palm frond base ash concrete.

Figure 4. Vicat apparatus for setting time test

3.2. Fresh Test

The workability of fresh concrete mixes was assessed using the slump test, Fig. 5, and the measurements were conducted following ASTM C 143[20].

Figure 5. Slump test

3.3. Hardened Concrete Tests

3.3.1. Compressive Strength Test

The compressive strength test has been measured depending on BS EN 12390-3 [21]. Three cubes with dimensions of (100×100×100)mm were tested at ages of 7, 28, and 90 days. Fig. 6 shows the test work.

Figure 6. Compressive strength test

3.3.2. Splitting Tensile Strength Test

The splitting tensile strength was determined according to ASTM C496 [22]; three cylinders of (100×200) mm were tested at ages 7, 28, and 90 days, as shown in Fig. 7.

Figure 7. Splitting tensile strength test

3.3.3. Static Modulus of Elasticity Test

This test was carried out on three (100×200) mm cylindrical specimens. According to ASTM C469 [23], as shown in Fig. 8.

Figure 8. Static modulus of elasticity test

3.3.4. Ultrasonic Pulse Velocity Test

The ultrasonic pulse velocity was measured using Pundit Lab+ for concrete, three cubes of (100x100) mm at 28 days. The test was implemented according to ASTM C597 [24], as shown in Fig. 9.

Figure 9. Ultrasonic pulse velocity test

3.3.5 Oven Dry Density Test

The oven dry density was determined according to ASTM C1754 [25] by drying three cubical specimens (100x100) mm at 150±2 C° for 24 hours, then they were cured in water for 28 days, and then the weight was measured.

3.3.6 Scanning Electron Microscope (SEM)

For the investigation of the concrete's microstructure, small pieces from the broken cubes used in the compressive strength test were subjected to SEM analysis. This analysis was carried out for both the control mix and the mix with 20% PFA replacement at 28 and 90 days, and a 2000 magnification was used for the analysis to know the changes and developments that occurred in the texture of the concrete due to the incorporation of palm ash, and compare it with the reference mix. following the procedures specified in ASTM C1723[26].

3.4 Durability Tests

The water absorption and sorptivity tests were conducted using three 100 mm cubes after a 28-day curing period, following the standards outlined in ASTM C642 [27] and ASTM C1585 [28], respectively. Fig. 10 shows the sorptivity test.

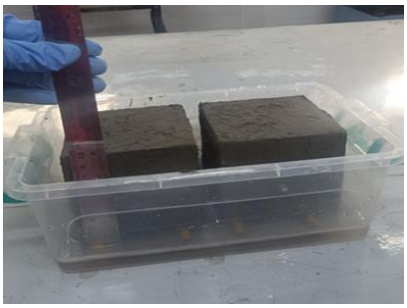

Figure 10. Sorptivity test

4. Results and Discussion

4.1 Setting Time

Initial and final setting times are plotted in Fig. 11 and Fig. 12 for PFA and PFAB replacement, respectively. As can be seen, the higher the replacement level for both types of ashes, the higher the initial and final setting. The reason was that the palm ash is siliceous in nature, and the reaction of silica is slow because it interacts with $Ca(OH)_2$ released from the hydration products, so the relationship between the setting time and the increase in PFA and PFAB replacement is a direct relationship [29].

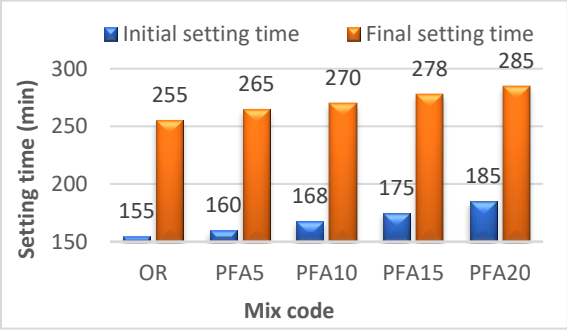

Figure 11. Setting time for palm frond ash

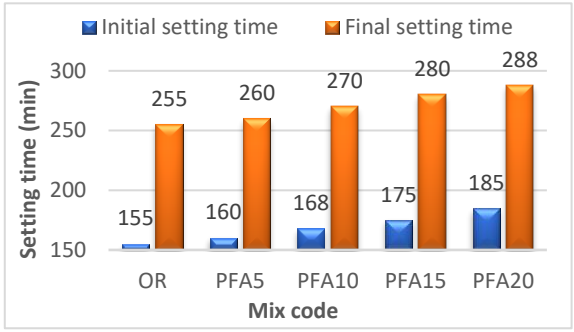

Figure 12. Setting time for palm frond base ash

4.2. Slump

Fig. 13 illustrates a decline in the slump as the level of replacement rises for both PFA and PFAB replacement. However, it's worth noting that PFA20 and PFBA20 mixes showed particularly low slump levels. This increase in water requirements can be attributed to the shape and characteristics of the palm ash particles. The angular and irregular shape of these particles necessitates more water to lubricate their surfaces. Additionally, since palm ash particles are porous in nature, they tend to absorb more water, thereby reducing the slump values [30]. Also, the results in Table 1 indicate that the Blain fineness for the PFA and PFBA was higher than that of cement, so the water demands are higher than those of cement due to increased surface area for the PFA and PFBA.

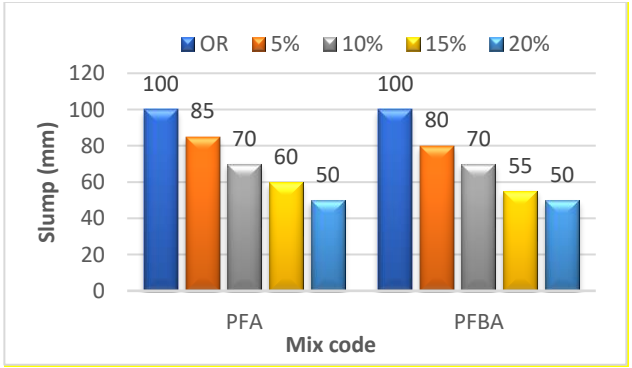

Figure 13. Slump for palm frond ash and palm frond base ash replacement

4.3. Compressive Strength Test

As shown in Fig. 14 and Fig. 15, at early ages (7 days), the compressive strength of PFA and PFBA-concrete decreased with an increasing replacement ratio. This decrease continued at 28 days, except that PFA5 had a higher compressive strength than the control mix, but the rate of increase in compressive strength for all the replacement ratios from 7 to 28 days was higher than that of the rate of increase in compressive strength for the control mix. After 90 days, there was a significant increase in compressive strength, with all replacement mixes surpassing the compressive strength values of the control mix.

The reason for the development of compressive strength over time is attributed to the presence of silica and alumina in PFA and PFBA, which react with the $Ca(OH)_2$ created when moisture is present during cement hydration. This process creates more calcium silicate hydrate (C-S-H), which would fill the pores, thus improving compressive strength. But this reaction is slow, and this explains why compressive strength does not develop with increasing replacement levels at the early ages of 7 and 28 days. So the compressive strength increases with age, particularly after 90 days [31]. These results are compatible with the results obtained by [29], which show that the strength gain was linear with the curing period. The slight difference in compressive strength between concrete with PFA replacement and concrete with PFBA replacement can be attributed to the higher percentage of silica and alumina in PFA compared to PFBA.

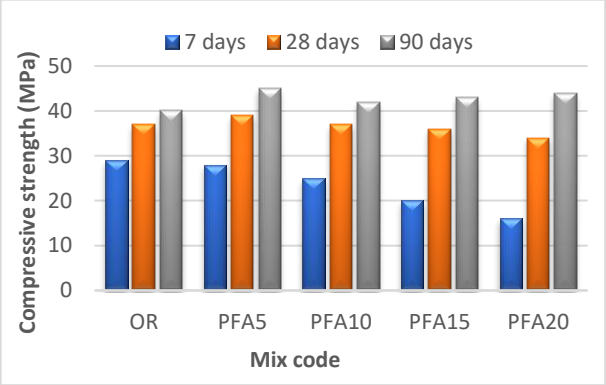

Figure 14. Compressive strength for palm frond ash replacement

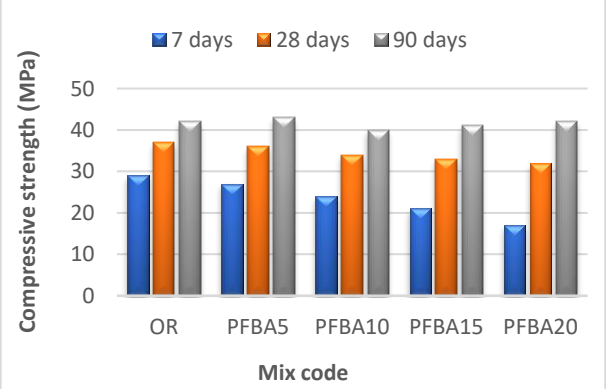

Figure 15. Compressive strength for palm frond base ash replacement

4.4. Splitting Tensile Strength

Examining the values for splitting tensile and strength in Fig. 16 and Fig. 17 reveals a decrease in this property as the replacement ratio of PFA and PFBA increases at the age of 7 days. However, at the age of 28 days, PFA concrete exhibited higher splitting tensile strength than the control mix for all replacement ratios, while PFBA concrete showed slightly lower splitting tensile strength than the control mix for all replacement ratios. After 90 days, there was a noticeable increase in splitting tensile strength for all replacement ratios in both PFA and PFBA mixes, with all replacement mixes surpassing the control mix. The highest values were observed for PFA5 and PFBA5.

The explanation for this behavior is the same as described for compressive strength. The creation of C-S-H, which arises from the interaction between silica found in (PFA) and (PFBA) and $Ca(OH)_2$ released from hydration products, fills voids and macro-cracks that are primarily responsible for initiating splitting tensile failure [32]. This interaction starts slowly at an early age and becomes more pronounced as the curing period extends.

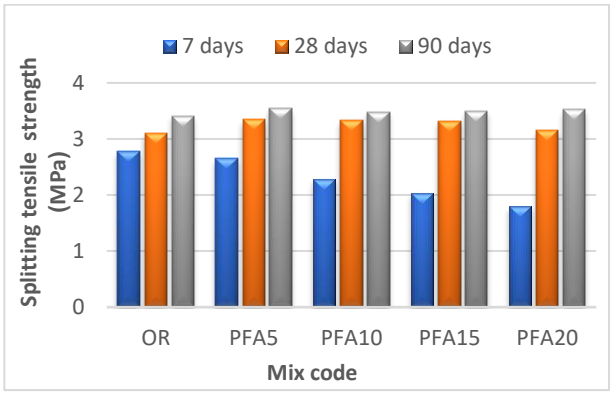

Figure 16. Splitting tensile strength for palm frond ash replacement

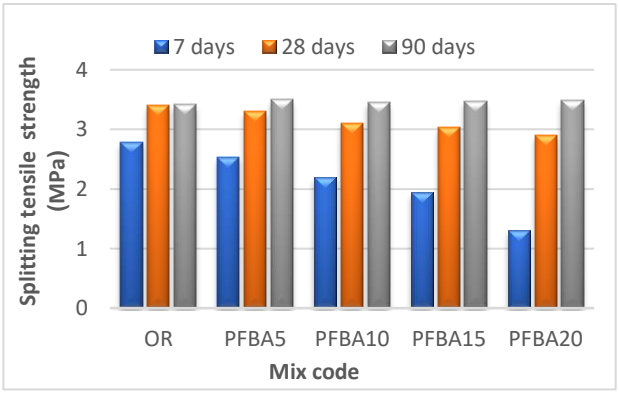

Figure 17. Splitting tensile strength for palm frond base ash replacement

4.5. Static Modulus of Elasticity

When concrete is under a load, it demonstrates a linear stress-strain relationship within the elastic range. This ratio signifies the slope of this linear segment, which is known as the modulus of elasticity. The elastic limit is defined as "the maximum stress a material can withstand without deviating from the proportionality of stress to strain according to Hooke's law"[33].

The effects of PFA and PFBA on the modulus of elasticity of concrete mixes are illustrated in Fig. 18 and Fig. 19. For both PFA and PFBA-concrete, the 7-day modulus of elasticity for all

mixes was lower than that for the control mix and decreased as the replacement ratio increased. However, at 28 days, the PFA5 and PFBA5 mixes exhibited a modulus of elasticity higher than that of the control mix. Beyond the 5% replacement level, the modulus of elasticity values decreased with an increase in ash content.

After 90 days, there was a noticeable increase in the modulus of elasticity for all replacement percentages in both PFA and PFBA mixes. In fact, all replacement mixes outperformed the control mix in terms of modulus of elasticity.

As discussed previously, the reaction between $Ca(OH)_2$ released during the cement hydration process and SiO_2 present in PFA and PFBA, along with water, leads to a pozzolanic reaction that produces new C–S–H. This product has a positive impact on the interfacial transition zone between the aggregates and cement paste, resulting in enhanced compressive strength and, consequently, increased stiffness of the concrete[34].

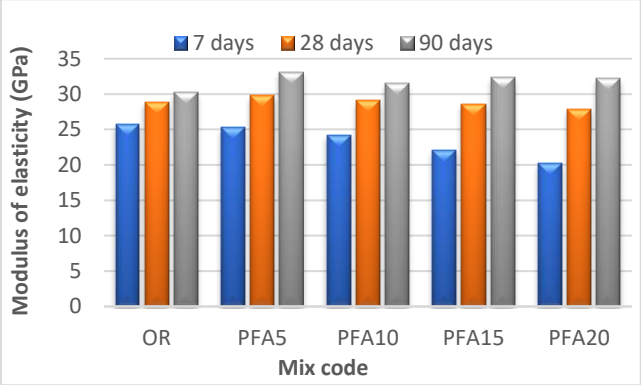

Figure 18. Modulus of elasticity for palm frond ash replacement

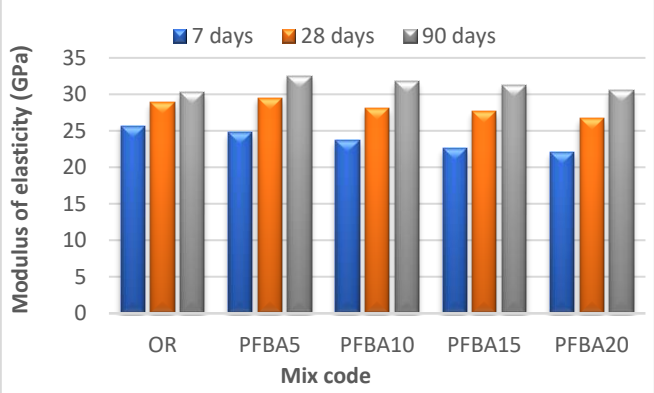

Figure 19. Modulus of elasticity for palm frond base ash replacement

4.6. Oven Dry Density and Ultrasonic Pulse Velocity

The average results of oven dry density (ODD) are shown in Fig. 20. They ranged from 2378 to 2339 kg/m3 and 2380 to 2309 kg/m3 for PFA and PFBA concrete, respectively. The PFA5 and PFBA5 mixes gave the highest values, even higher than the control mix, and then the ODD started to reduce with an increment in the replacement level of ash, irrespective of its type. This reduction in ODD might be related to two reasons: first, the PFA and PFBA had a specific gravity lower than OPC, which would reduce the magnitude of density, and second, due to the potential of the PFA and PFBA to trap air bubbles [35].

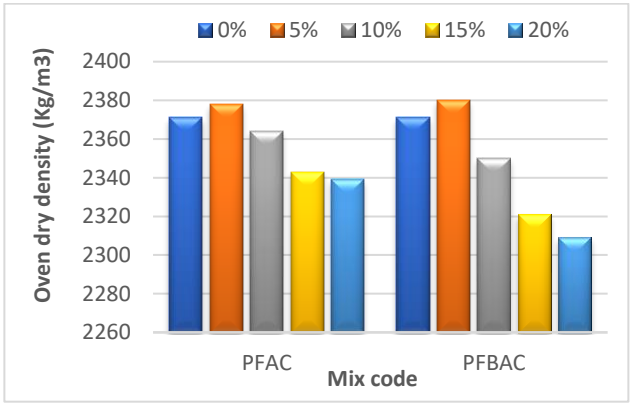

Figure 20. Oven dry density for Palm Front ash and Palm frond base ash replacement

As for ODD, ultrasonic pulse velocity (UPV) was monitored for 28 days, and the results are illustrated in Fig. 21. Similar to the density results, the PFA5 and PFBA5 mixes showed the best UPV, and as the ash content increased beyond 5%, the UPV started to decrease. UPV is an indication of the quality of concrete, and it can be categorized as excellent if UPV is >4.5 km/s, good (3.5–4.5 km/s), medium (3–3.5 km/s), or poor (<3 km/s) [36]. The UPV recorded for the mixes with ash varied from 4.807 to 4.761 km/s for PFA inclusion and varied from 4.820 to 4.675 km/s for PFBA inclusion, so the concrete quality for all replacements and for both types of ash was excellent. This could be attributed to the fact that UPV is considered to be related to the density of concrete; when the density declines, there is a high percentage of voids and thus less UPV, since the UPV value is strongly related to the presence of voids in concrete[8].

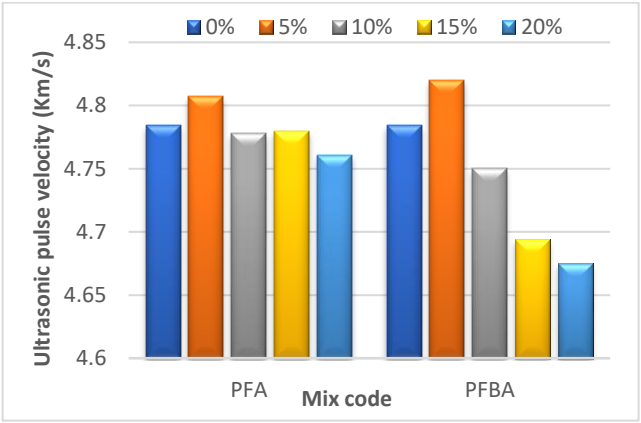

Figure 21. Ultrasonic pulse velocity for Palm Frond and ash, and Palm Frond Base Ash Replacement

4.7. Scanning Electron Microscope (SEM)

Fig. 22 displays typical micrographs for the selected mixes with and without palm frond ash. It is evident that the microstructure of the control mix and the PFA20- concrete contains ettringite

needles, voids, and C-S-H gel in the cement paste. After curing for an age of 90 days, Fig. 22 (b) shows that although the control mix concrete's microstructure has improved, some voids and ettringite needles are still present. In contrast, PFA20-concrete is denser and free of voids and ettringite needles at 90 days (Fig. 22(d)) than the control mix. This phenomenon is due to (C-S-H) formation resulting from the interaction between silica in PFA and calcium hydroxide ($Ca(OH)_2$). This interaction fills voids and strengthens the concrete's microstructure [37].

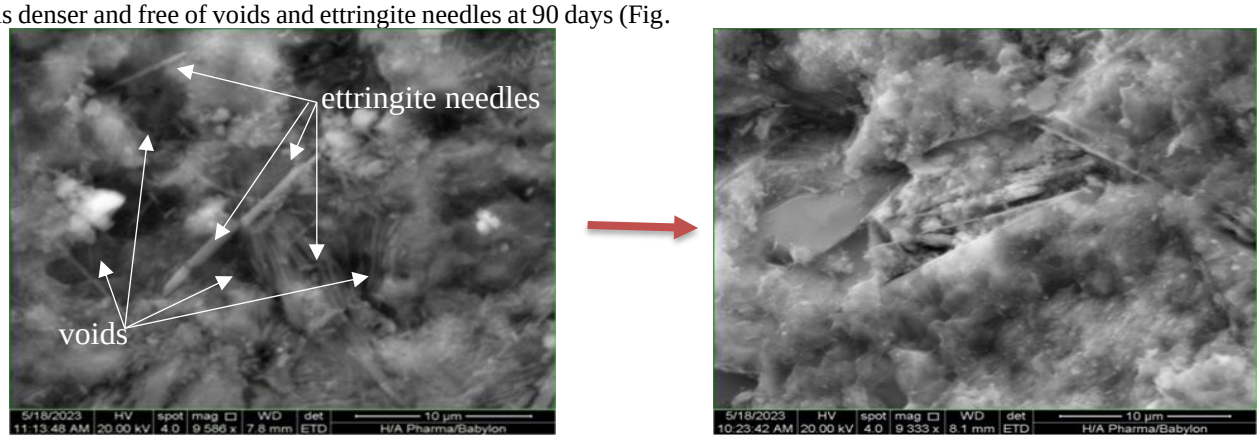

(a) SEM for control mix at 28 days

(b) SEM for control mix at 90 days

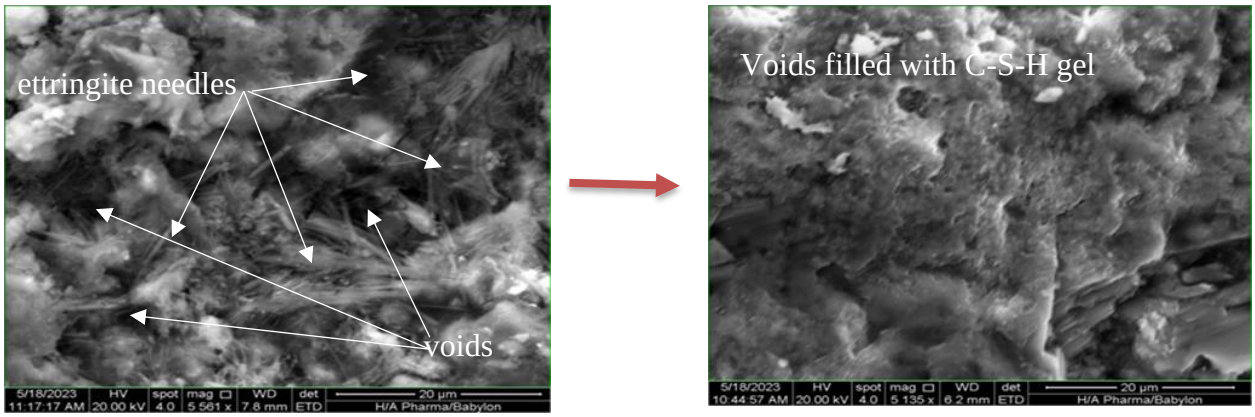

(c) SEM for PFA20-concrete at 28 days

(d) SEM for PFA20-concrete at 90 days

Figure 22. SEM micrograph

4.8. Water Absorption and Sorptivity

Concrete with water absorption of less than 3% is categorized as "good," while concrete with 3-5% water absorption is categorized as "average." Concrete with more than 5% water absorption can be categorized as "poor"[38]. Upon examining the data on water absorption presented in Fig. 23, it can be concluded that all the investigated concrete samples are classified as "good" since they recorded water absorption of less than 3%.

The results of water absorption and sorptivity are summarized in Fig. 23 and Fig. 24. They reveal that at 28 days, the mix with a 5% replacement level of PFA exhibited the lowest water absorption and sorptivity. In contrast, all the other mixes displayed higher values in comparison to the control mix.

Considering the replacement ratio for both PFA and PFBA increases, the concrete's density decreases. Consequently, this results in an increase in pores, particularly interconnected ones. This, in turn, leads to a significant increment in both water absorption and sorptivity[39].

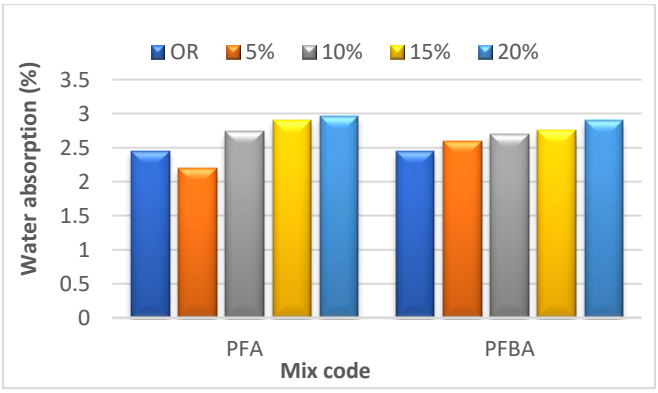

Figure 23. Water absorption for palm frond ash and palm front base ash replacement

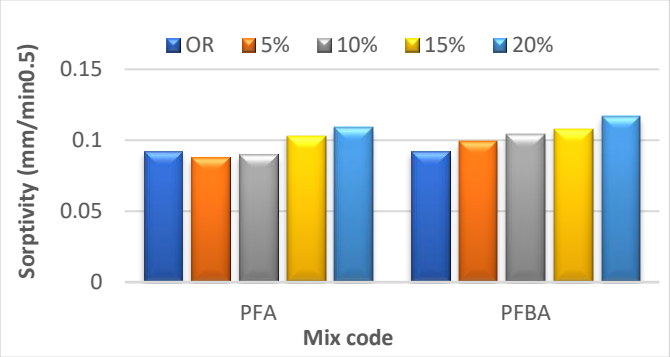

Figure 24. Sorptivity for palm frond ash and palm front base ash replacement

5. Conclusions

The study's findings provide several noteworthy conclusions. Firstly, increasing the replacement ratio of (PFA) and (PFBA) led to extended initial and final setting times, with the highest replacement level resulting in the longest setting time. Additionally, the slump reduced as replacement rose, with PFA20 and PFBA20 replacements resulting in lower slump levels. Although there was a small decline in Compressive and splitting tensile strength at 7 days due to palm ash inclusion, these properties showed a subsequent improvement, surpassing control mixes without ash. The 7-day elastic modulus declined with higher palm ash replacement, but after 28 days of water curing, PFA5, PFBA5, and PFA10 mixes outperformed the control mix, with all other mixes demonstrating greater stiffness than the control mix at 90 days. The optimal oven-dry density at 28 days was observed in PFA5 and PFBA5, beyond which there was a density reduction. Ultrasonic Pulse Velocity, closely related to concrete density, exhibited a similar trend. SEM tests revealed a microstructure improvement over time, particularly when compared to the control mix. Notably, PFA5 exhibited lower water absorption and sorptivity than the control mix at 28 days, indicating enhanced durability and performance.

Conflict of interest

The authors affirm that there will be no conflict of interest as a result of publishing this article.

Author Contribution Statement

Safa Alqeisi conducted the experiments, coordinated the organization, and documented the results.

Ali H. Nahhab formulated the research problem and supervised the investigation and its outcomes.

Both authors discussed the results and contributed to the final manuscript.

References

[1] D. Oyejobi, T. Abdulkadir, and A. Ahmed, "A study of partial replacement of cement with palm oil fuel ash in concrete production," *Journal of Agricultural Technology*, vol. 12, no. 4, pp. 619–631, 2015. doi: http://dx.doi.org/10.5281/zenodo.192492.

[2] C. Chen, R. Xu, D. Tong, X. Qin, J. Cheng, J. Liu, et al., "A striking growth of CO_2 emissions from the global cement industry driven by new facilities in emerging countries," *Environmental Research Letters*, vol. 17, no. 4, art. no. 044007, 2022. doi: https://doi.org/10.1088/1748-9326/ac48b5.

[3] M. Nasir and W. Al-Kutti, "Performance of date palm ash as a cementitious material by evaluating strength, durability, and characterization," *Buildings*, vol. 9, no. 1, art. no. 6, 2018. doi: https://doi.org/10.3390/buildings9010006.

[4] S. A. Zaimi, M. N. Muhd Sidek, N. H. Hashim, H. Mohd Saman, R. Putra Jaya, and N. A. Marzuki, "Potential of palm oil fuel ash as a partial replacement of fine aggregates for improved fresh and hardened mortar performance," *Advances in Civil Engineering*, vol. 2023, art. ID 9064645, 2023. doi: https://doi.org/10.1155/2023/9064645.

[5] M. Ayub, M. H. D. Othman, I. U. Khan, S. K. Hubadillah, T. A. Kurniawan, A. F. Ismail, and J. Jaafar, "Promoting sustainable cleaner production paradigms in palm oil fuel ash as an eco-friendly cementitious material: A critical analysis," *Journal of Cleaner Production*, vol. 295, art. no. 126296, 2021. doi: https://doi.org/10.1016/j.jclepro.2021.12629.

[6] H. M. Hamada, G. A. Jokhio, F. M. Yahaya, A. M. Humada, and Y. Gul, "The present state of the use of palm oil fuel ash (POFA) in concrete," *Construction and Building Materials*, vol. 175, pp. 26–40, 2018. doi: https://doi.org/10.1016/j.conbuildmat.2018.03.227.

[7] M. Z. Al-mulali, H. Awang, H. A. Khalil, and Z. S. Aljoumaily, "The incorporation of oil palm ash in concrete as a means of recycling: A review," *Cement and Concrete Composites*, vol. 55, pp. 129–138,2015.doi: https://doi.org/10.1016/j.cemconcomp.2014.09.007.

[8] H. M. Hamada, A. Alya'a, F. M. Yahaya, K. Muthusamy, B. A. Tayeh, and A. M. Humada, "Effect of high-volume ultrafine palm oil fuel ash on the engineering and transport properties of concrete," *Case Studies in Construction Materials*, vol. 12, art. no. e00318, 2020. doi: https://doi.org/10.1016/j.cscm.2019.e00318.

[9] M. O. Yusuf, "Strength and microstructure of alkali-activated binary blended binder containing palm oil fuel ash and ground blast-furnace slag," *Construction and Building Materials*, vol. 52, pp. 504–510,2014.doi: https://doi.org/10.1016/j.conbuildmat.2013.11.012.

[10] S. N. Chinnu, S. N. Minnu, A. Bahurudeen, and R. Senthilkumar, "Influence of palm oil fuel ash in concrete and a systematic comparison with widely accepted fly ash and slag: A step towards sustainable reuse of agro-waste ashes," *Cleaner Materials*, art. no. 100122, 2022. doi: https://doi.org/10.1016/j.clema.2022.100122.

[11] P. Topark-Ngarm, P. Chindaprasirt, and V. Sata, "Setting time, strength, and bond of high-calcium fly ash geopolymer concrete," *Journal of Materials in Civil Engineering*, vol. 27, no. 7, art. no. 04014198, 2014.doi: https://doi.org/10.1061/(ASCE)MT.1943-5533.0001157.

[12] B. S. Thomas, S. Kumar, and H. S. Arel, "Sustainable concrete containing palm oil fuel ash as a supplementary cementitious material—A review," *Renewable and Sustainable Energy Reviews*, vol. 80, pp. 550–561,2017.doi: https://doi.org/10.1016/j.rser.2017.05.128.

[13] F. A. Hadi, H. Awang, and M. Z. Almulali, "The effect of oil palm ash incorporation in foamed concrete," *Jurnal Teknologi (Sciences & Engineering)*, pp. 63–68, 2015.

[14] Iraqi Quality and Standards (IQS), *Iraqi Specifications No. (5): f.P.C.*, ICS: 91.100.10, Baghdad, Iraq, 2019.

[15] Iraqi Quality and Standards (IQS), *Iraqi Specifications No. (45): Aggregate from Natural Sources for Concrete and Building Construction*, Baghdad, Iraq, 1984.

[16] ASTM C188-17, *Standard Test Method for Density of Hydraulic Cement*, ASTM International, West Conshohocken, PA, USA, 2017. doi: https://doi.org/10.1520/c0188-17r23.

[17] American Concrete Institute (ACI), *ACI PRC-211.1-22: Selecting Proportions for Normal-Density and High-Density Concrete*, Farmington Hills, MI, USA, 2022.[Online].Available https://www.concrete.org/store/productdetail.aspx?ItemID=211122&Language=English&Units=US_AND_METRIC.

[18] ASTM C187-11, *Standard Test Method for Amount of Water Required for Normal Consistency of Hydraulic Cement Paste*, ASTM International, West Conshohocken, PA, USA, 2011. doi: https://doi.org/10.1520/c0187-11e01.

[19] ASTM C191-13, *Standard Test Methods for Time of Setting of Hydraulic Cement by Vicat Needle*, ASTM International, West Conshohocken, PA, USA, 2013. doi: https://doi.org/10.1520/c0191-13.

[20] ASTM C143/C143M-15a, *Standard Test Method for Slump of Hydraulic-Cement Concrete*, ASTM International, West Conshohocken, PA, USA, 2015. doi: https://doi.org/10.1520/c0143_c0143m-15a.

[21] BS EN 12390-3:2019, *Testing Hardened Concrete—Part 3: Compressive Strength of Test Specimens*, BSI Standards Publication, London, UK, 2019. doi: https://doi.org/10.3403/30360097.

[22] ASTM C496/C496M-11, *Standard Test Method for Splitting Tensile Strength of Cylindrical Concrete Specimens*, ASTM International, West Conshohocken, PA, USA, 2011. doi: https://doi.org/10.1520/c0496_c0496m-11.

[23] ASTM C469/C469M-14, *Standard Test Method for Static Modulus of Elasticity and Poisson's Ratio of Concrete in Compression*, ASTM International, West Conshohocken, PA, USA, 2014. doi: https://doi.org/10.1520/c0469_c0469m-14.

[24] ASTM C597-09, *Standard Test Method for Pulse Velocity Through Concrete*, ASTM International, West Conshohocken, PA, USA, 2009. doi: https://doi.org/10.1520/c0597-09.

[25] ASTM C1754/C1754M-12, *Standard Test Method for Density and Void Content of Hardened Pervious Concrete*, ASTM International, West Conshohocken, PA, USA, 2012. doi: https://doi.org/10.1520/c1754_c1754m-12.

[26] ASTM C1723-10, *Standard Guide for Examination of Hardened Concrete Using Scanning Electron Microscopy*, ASTM International, West Conshohocken, PA, USA, 2010. doi: https://doi.org/10.1520/c1723-10.

[27] ASTM C642-13, *Standard Test Method for Density, Absorption, and Voids in Hardened Concrete*, ASTM International, West Conshohocken, PA, USA, 2013. doi: https://doi.org/10.1520/c0642-13

[28] ASTM C1585-13, *Standard Test Method for Measurement of Rate of Absorption of Water by Hydraulic Cement Concretes*, ASTM International, West Conshohocken, PA, USA, 2013. doi: https://doi.org/10.1520/c1585-13

[29] M. Nasir, W. Al-Kutti, T. S. Kayed, A. Adesina, and T. Chernykh, "Synthesis and SWOT analysis of date palm frond ash–Portland cement composites," *Environmental Science and Pollution Research*, vol. 28, pp. 45240–45252, 2021. doi: https://doi.org/10.1007/s11356-021-13957-9

[30] E. K. K. Nambiar and K. Ramamurthy, "Influence of filler type on the properties of foam concrete," *Cement and Concrete Composites*, vol. 28, pp. 475–480, 2006. doi: https://doi.org/10.1016/j.cemconcomp.2005.12.001

[31] A. M. Alnahhal, U. J. Alengaram, S. Yusoff, R. Singh, M. K. Radwan, and W. Deboucha, "Synthesis of sustainable lightweight foamed concrete using palm oil fuel ash as a cement replacement material," *Journal of Building Engineering*, vol. 35, art. no. 102047, 2021. doi: https://doi.org/10.1016/j.jobe.2020.102047.

[32] A. M. Neville and J. J. Brooks, *Concrete Technology*, Longman Scientific & Technical, England, 1987, p. 438.

[33] B. Haranki, *Strength, Modulus of Elasticity, Creep and Shrinkage of Concrete Used in Florida*, M.Sc. thesis, University of Florida, Gainesville, FL, USA, 2009, p. 176.[Online].Available http://ufdcimages.uflib.ufl.edu/UF/E0/02/45/06/00001/haranki_b.pdf.

[34] M. Amran, G. Murali, R. Fediuk, N. Vatin, Y. Vasilev, and H. Abdelgader, "Palm oil fuel ash-based eco-efficient concrete: A critical review of the short-term properties," *Materials*, vol. 14, no. 2, art. no. 332, 2021. doi: https://doi.org/10.3390/ma14020332.

[35] N. Ranjbar, A. Behnia, B. Alsubari, P. M. Birgani, and M. Z. Jumaat, "Durability and mechanical properties of self-compacting concrete incorporating palm oil fuel ash," *Journal of Cleaner Production*, vol. 112, pp. 723–730, 2016. doi: https://doi.org/10.1016/j.jclepro.2015.07.033.

[36] IS 13311:1992, *Method of Non-Destructive Testing of Concrete—Part 1: Ultrasonic Pulse Velocity*, Bureau of Indian Standards, pp. 1–7, 1992.

[37] A. Salam, M. Safiuddin, and Z. B. Jumaat, "Mechanical properties and microstructure of self-consolidating high-strength concrete including palm oil fuel ash," *ACI Materials Journal*, vol. 119, no. 1, 2022. doi: https://doi.org/10.14359/51732982.

[38] D. Manikanta and D. P. Ravella, "Mechanical and durability characteristics of high-performance self-compacting concrete containing fly ash, silica fume, and graphene oxide," *Materials Today: Proceedings*, vol. 43, pp. 2361–2367, 2021. doi: https://doi.org/10.1016/j.matpr.2021.01.684.

[39] M. Y. J. Liu, U. J. Alengaram, M. Santhanam, M. Z. Jumaat, and K. H. Mo, "Microstructural investigations of palm oil fuel ash and fly ash-based binders in lightweight aggregate foamed geopolymer concrete," *Construction and Building Materials*, vol. 120, pp. 112–122, 2016. doi: https://doi.org/10.1016/j.conbuildmat.2016.05.076.